

# Measuring many-body effects in carbon nanotubes with a scanning tunneling microscope

H. Lin,<sup>1,2</sup> J. Lagoute,<sup>1</sup> V. Repain,<sup>1</sup> C. Chacon,<sup>1</sup> Y. Girard,<sup>1</sup> J.-S. Lauret,<sup>3</sup> F. Ducastelle,<sup>2</sup> A. Loiseau,<sup>2</sup> and S. Rousset<sup>1</sup>

<sup>1</sup>Laboratoire Matériaux et Phénomènes Quantiques, Université Paris Diderot, CNRS, UMR7162, 10 rue Alice Domon et Léonie Duquet, 75205 Paris Cedex 13, France

<sup>2</sup>Laboratoire d'Etude des Microstructures, ONERA-CNRS, BP72, 92322 Châtillon, France

<sup>3</sup>Laboratoire de Photonique Quantique et Moléculaire, Institut d'Alembert, Ecole Normale Supérieure de Cachan, 94235 Cachan Cedex, France

(Dated: July 2, 2009)

Electron-electron interactions and excitons in carbon nanotubes are locally measured by combining Scanning tunneling spectroscopy and optical absorption in bundles of nanotubes. The largest gap deduced from measurements at the top of the bundle is found to be related to the intrinsic quasi-particle gap. From the difference with optical transitions, we deduced exciton binding energies of 0.4 eV for the gap and 0.7 eV for the second Van Hove singularity. This provides the first experimental evidence of substrate-induced gap renormalization on SWNTs.

PACS numbers: 78.67.Ch,73.22.-f,71.35.Cc,68.37.Ef

The electronic properties of single-walled carbon nanotubes (SWNT) have attracted wide interest since their discovery. The tunability from metallic to semiconducting character through a structural control makes them promising candidates for the development of molecular electronics. It is therefore crucial to understand and control their electronic properties down to the atomic scale. Scanning tunneling microscopy (STM) and spectroscopy (STS) are powerful tools for the local investigation of 1D band structure of SWNTs and of its link to the atomic structure [1, 2, 3]. STS experiments have been successfully interpreted within a simple tight-binding zone-folding scheme which shows a density of states dominated by a series of Van-Hove singularities [4, 5]. The energy separation between the first two singularities on each side of the Fermi level is denoted  $E_{11}^S$  for semiconducting tubes and  $E_{11}^M$  for metallic tubes. The simplest tight-binding model gives a relation between the electronic gap  $E_{11}^S$  and the tube diameter  $d$ ,  $E_{11}^S = 2\gamma_0 a_{c-c}/d$  where  $a_{c-c}$  is the carbon-carbon distance (1.42 Å) and  $\gamma_0$  is the hopping integral between first neighbours, ranging from 2.5 [6] to 2.9 eV [7]. Although the tight-binding model captures the main features of the electronic structure of nanotubes [8], many-body effects play a role in 1D systems and significantly modify the energy of the electronic transitions. Two main contributions should be taken into account: self-energy effects which modify the single-particle excitation spectrum and, in the case of optical transitions, excitonic electron-hole interactions [9, 10, 11, 12].

The major role of excitons in the optical transition of nanotubes has been demonstrated by using two-photon absorption experiments [13, 14, 15]. After this finding, the interpretation of subband transitions measured in optical experiments has been revisited. Although a parameterized tight-binding model could explain the so-called Kataura plot, it turned out that a complete description

should include many-body effects. Theoretical discussions show that self-energy and excitonic effects tend to cancel each other, both effects being of the same order of magnitude, in the range of 0.5 to 1 eV. The overall result is a weak blue shift effect [10, 16, 17].

In the same way, scanning tunneling microscopy results on SWNTs must be revisited to some extent. STM experiments are not expected to be sensitive to the electron-hole interaction and one expects the gap measured by STM to be larger than the optical one, the difference corresponding to the exciton binding energy. However, to perform STS measurements, the tubes are usually placed on a metallic substrate. Charge transfer between the metallic substrate and the tube shifts the Fermi level of the tube [18, 19]. In the case of molecules, the renormalization of the electronic gap by substrate-induced charging effects in STS measurements has been studied both theoretically and experimentally [20, 21, 22] and a similar effect is expected for SWNTs [16] although detailed experimental data are still lacking.

In this Letter, we provide experimental evidence of this substrate-induced gap renormalization on SWNTs. STS measurements show a systematic variation of the band gap measured on semi-conducting tubes, depending on whether the tube is on the top of a bundle or in direct contact with the metallic substrate. A single-particle model for  $E_{11}^S$  is not sufficient to account for the experimental data. On the other hand a quasi-particle model combined with an analysis of substrate-induced screening effects allows us to propose a consistent interpretation of our experiments. The unscreened gap deduced from STS measurements is later compared with the optical absorption spectrum providing us with a unique tool for determining the exciton binding energies.

STM/STS measurements were performed using a low temperature (5K) STM operating under UHV conditions ( $10^{-10}$  mbar). The nanotubes were synthesized by arc

discharge technique and deposited from a dispersion in alcohol after sonication onto a single-crystalline Au (111) surface previously cleaned in UHV by repeated cycles of ion argon sputtering and annealing at 800 K. The samples were dried in air and introduced into the UHV system. Although the preparation was aimed to avoid bundling of nanotubes, bundles are still observed after the deposition. All measurements were performed with tungsten tips. Optical absorption spectra were recorded with a spectrophotometer (lambda 900 Perkin-Elmer) on the same solution deposited onto a glass substrate.

The electronic gap of a nanotube is principally determined by its diameter. It is therefore crucial to have a precise knowledge of the diameter distribution of the nanotubes. Although STM allows us to attain atomic resolution, tip profile effects lead to a poor estimation of the tube diameters. To overcome that problem, we combined the STM investigation with transmission electron microscopy (TEM) analysis which, in contrast, can provide more accurate values of these diameters. Using a gaussian fit we obtain a statistical distribution centered at 1.4 nm with a FWHM of 0.2 nm. This distribution has been projected onto the Kataura plots (see Fig. 1) to deduce the induced gap distributions.

Fig.1 displays first the plot deduced from the simplest linearized tight-binding model (lower curve),  $E_{11}^s = 2\gamma_0 a_{c-c}/d$ . Using  $\gamma_0 = 2.9$  eV, this plot predicts a gap distribution centred at 0.59 eV (see Fig. 1). The second plot is deduced from two-photon experiments [14] where the single-quasiparticle gap is expressed by  $E_{11}^s = 0.34/d + 1.11/(d + 0.11)$  (upper curve in Fig. 1). We now obtain a gap distribution centered at 0.98 eV. The difference between the two curves corresponds to the many-body self-energy contributions. The upper curve will be referred as “many-body” gap, even if it should be kept in mind that excitonic effects are not included [14].

Because of the narrowness of the diameter distribution, the simple tight-binding and the many-body gap distributions do no overlap. It is then crucial to understand which one corresponds to the value measured in a STM experiment. We argue hereafter that, to some extent, and depending on the tube-substrate separation, both are measured. After deposition on the Au(111) substrate, most nanotubes arrange into bundles. The differential conductance image at 12 mV (see Fig. 2(a)) shows the distribution of the local density of state around the Fermi level and allows us to separate clearly the metallic (bright) and semi-conducting tubes (black) in the image. Fig. 2(b) shows typical  $dI/dV$  spectra measured on the substrate and on the tubes. On the gold substrate, the differential conductance has a constant non-zero value as expected (black dashed curve). On the nanotubes, spectra are dominated by Van-Hove singularities. On the metallic tube, the conductance between the two first singularities is close to that of the substrate, except for a dip around the Fermi level (dotted curve). This pseudo-

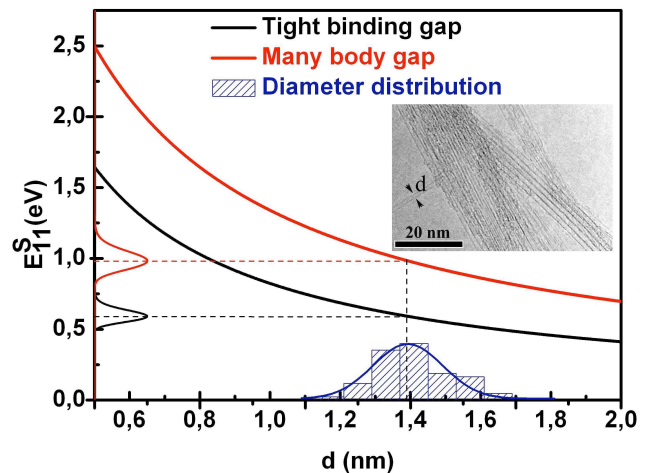


FIG. 1: (Color online) Statistic distribution of nanotubes diameter measured on TEM images of 50 SWNTs (Philips CM20, 200 kV). The inset presents an example of a TEM image. The lower and upper curves are the  $E_{11}^s$  gap using the single-particle tight-binding model or the many body values [14], respectively. The corresponding gap distributions are shown on the vertical axis.

gap was observed for all the metallic tubes investigated. It is known to be due to curvature effects or intertube interactions and has already been observed [23].

Two spectra of semi-conducting tubes showing the first two Van-Hove singularities are presented in Fig. 2(b). The peak positions are not symmetric with respect to the Fermi level, which is due to tube-substrate charge transfer [1, 2, 3]. The energy subband separations  $E_{11}^S$  are measured at the point of maximum slope in the peak. The values when the tube directly contacts the substrate (tube 1) or is at the top of the bundle (tube 2) are equal to 0.70 eV (green spectrum) and 0.91 eV (red spectrum) respectively (Fig. 2(b)). It is worth noticing that we did not measure similar variations of the  $E_{11}^M$  transition for metallic tubes. As shown in Fig.1, the dispersion in the gap values of semiconductor tubes cannot be accounted for by the width of the diameter distribution within one or the other model. On the other hand the gap of the tube contacting the metal compares well with the gap given by the single-particle model, while the gap of the tube separated from the substrate by the bundle lies within the distribution estimated by the “many-body” Kataura plot. The transition between these two situations can be understood considering the potential image effect which decreases when the tube-sample distance increases. Within this model the  $E_{11}^S$  transition of a nanotube adsorbed on a metal corresponds to the gap of the free nanotube (including electron-electron interactions) reduced by the screening energy due to the image charge in the metal  $C_0 e^2/2D$ , where  $D$  is the tube-substrate distance and  $C_0 = 1/4\pi\epsilon_0$  [20, 22]. It is therefore expected

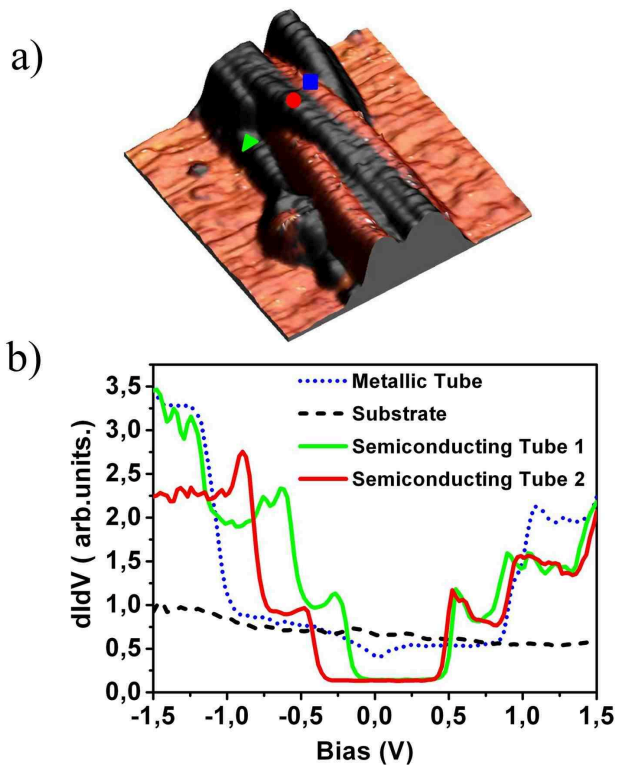


FIG. 2: (Color online) STM/STS of a bundle of tubes on the metallic surface. a) 3D view of the topographic image ( $40 \times 40 \text{ nm}^2$ ) with a color scale corresponding to the differential conductance image at 12 mV (black for low value, light gray (yellow online) for high value). b)  $dI/dV$  spectra taken at positions indicated in a).

that a nanotube separated from the metallic substrate has a larger gap than a nanotube in contact. In our experiment the bundle plays the role of a spacer which offers the possibility to measure the gap of semiconducting nanotubes at various tube-substrate separations. The largest gap measured at high height should then correspond to the genuine intrinsic quasi-particle gap of the nanotubes. To verify this hypothesis, we present in Fig. 3 the first and second subband energy separation as a function of the apparent height ( $h_a$ ) with respect to the gold substrate of several nanotubes as determined from STM images at 1 V. We see that for both the first and second singularities, the energy separation ( $E_{11}^S$  and  $E_{22}^S$ , respectively) tends to increase with the apparent height. The image charge model ( $E = E_0 - C_0 e^2 / (2h_a)$ ) fits reasonably well the experimental data (Fig. 3, dotted curves).

This first approach however does not consider the effective dielectric constant of the tube environment, neither the fact that the apparent height is not exactly equal to the tube-substrate distance. For these reasons we provide empirical fits using  $E = E_0 - C_1 e^2 / (2h_a)$ , where  $C_1 = 0.52C_0$  for the  $E_{11}$  gap and  $E = E_0 - C_2 e^2 / (2h_a)$  with  $C_2 = 0.89C_0$  for the  $E_{22}$  separation (solid lines in Fig. 3). Note that  $C_1 \neq C_2$  what is ascribed to many-

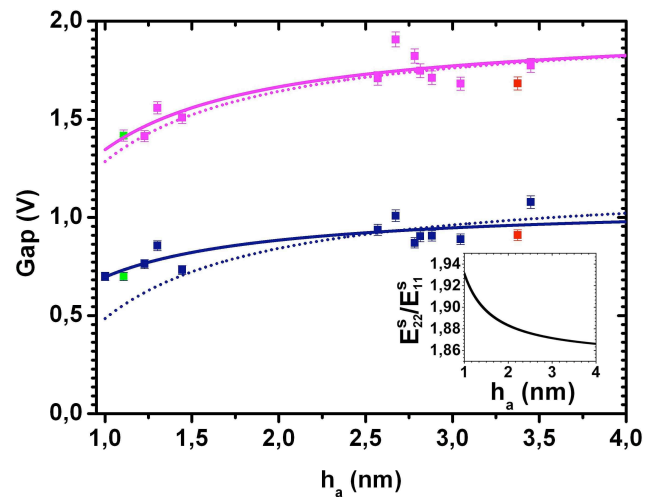


FIG. 3: (Color online) Gap as a function of the apparent height ( $h_a$ ) of the tubes. The squares are the experimental data. The dotted lines are fits using image charge model. The solid lines are fits using effective parameters  $C_1$  and  $C_2$ . The inset shows the  $E_{22}^S/E_{11}^S$  ratio. The green and red squares correspond to the tubes 1 and 2 of Fig. 2, respectively. The error bars are estimated from the diameter dispersion projected onto the tight-binding gap curve.

body effects, as discussed later. When  $h_a \rightarrow \infty$ ,  $E_0$  for the first and the second singularities tends to 1.1 eV and 2.0 eV, respectively. From our analysis, these values should therefore be equal to the quasi-particle gaps.  $E_{11}^S = 1.1$  eV is close to the gap deduced by the many-body relation with  $d=1.4$  nm (0.98 eV), and definitely larger than the tight-binding calculation (0.59 eV).

We now compare STS data with optical absorption spectrum of the same nanotubes sample displayed in Fig. 4. It is clear that the optical transitions occur at lower energies than those obtained in STS on the top of bundles (Fig. 3). The energy difference  $\Delta E$  between the optical transitions and the tunneling gap in the limit of infinite  $h_a$  is then a measure of the exciton binding energies. We obtain  $\Delta E_{11}^S = 0.4$  eV and  $\Delta E_{22}^S = 0.7$  eV. The  $E_{22}^S$  states have larger excitonic binding energy than  $E_{11}^S$  states, which is consistent with theoretical calculations [17, 24]. The  $\Delta E_{11}^S$  value obtained here is close to the binding energy determined in previous optical measurements where a law  $\Delta E_{11}^S \simeq 0.34/d$  has been derived [14]. Therefore combining STS with optical spectroscopy we can estimate the exciton binding energy of carbon nanotubes.

Finally, we discuss the  $E_{22}^S/E_{11}^S$  ratio measurement. This ratio is generally found experimentally smaller than 2 (about 1.8), the value provided by the simple linearized tight-binding model: this is the “ratio problem” [10]. It is now clear that the main explanation for this deviation is the effect of electron-electron interactions [10, 11], even if the relative contributions of self-energy and exci-

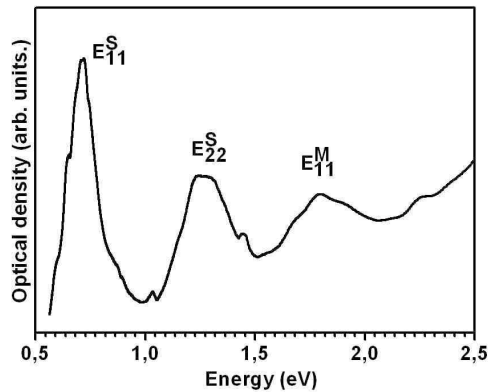


FIG. 4: (Color online) Optical absorption of SWNTs.  $E_{11}^S$ ,  $E_{22}^S$  and  $E_{11}^M$  are equal to 0.72, 1.26, and 1.79 eV respectively. The  $E_{22}^S/E_{11}^S$  ratio is equal to 1.75.

tonic effects are not precisely known. Calculations show also fairly large fluctuations of this ratio as a function of the chirality. In our STS experiments, sensitive to self-energy effects only, a  $E_{22}^S/E_{11}^S$  ratio close to 2 corresponds well to the left hand part of the curve in the inset of Fig.3, where the self-energy is largely compensated by the screening effect due to the image potential. As the tube-substrate distance increases, self-energy effects increase and the  $E_{22}^S/E_{11}^S$  ratio decreases gradually down to 1.85. Previous experimental data reported by Venema *et al.* [7] give a ratio close to 2, but their tubes lie on the metal, and according to our analysis, they correspond to a situation where self-energy effects are screened out. Considering now our optical absorption measurements, a lower  $E_{22}^S/E_{11}^S$  ratio about 1.75 is found. Our data indicate then that the gap ratio decreases when the screening of electron-electron interactions decreases.

To summarize, we used STS measurements to compare local spectroscopy of carbon nanotubes lying on a metallic substrate with the spectroscopy of nanotubes on top of bundles. We showed that the gap of a semiconducting tube increases when it is separated from the metal by a bundle, the gap variation being of the order of what is expected within an image charge model where self-energy effects are screened. The experimental conditions allowed us to observe a continuous transition from the almost totally screened case, to an almost intrinsic gap. By combining these data with optical absorption measurement, the exciton binding energies could then be estimated. In the case of 1.4 nm diameter nanotubes a mean value of 0.4 eV and 0.7 eV was found, for excitons corresponding to the  $E_{11}^S$  and  $E_{22}^S$  gaps. We believe that these measurements will open promising ways of determining locally the exciton binding energy of carbon nanotubes.

This study has been supported by the European Contract STREP “BCN” Nanotubes 30007654-OTP25763, by a grant of CNano IdF “SAMBA” and by the ANR project “CEDONA” of the PNANO programme (ANR-07-NANO-007.02). We gratefully acknowledge L. Henrard and P. Hermet for fruitful discussions.

- 
- [1] J. W. G. Wilder, L. C. Venema, A. G. Rinzler, R. E. Smalley, and C. Dekker, *Nature* **391**, 59 (1998).
  - [2] T. W. Odom, J.-L. Huang, P. Kim, and C. M. Lieber, *Nature* **391**, 62 (1998).
  - [3] L. C. Venema, V. Meunier, P. Lambin, and C. Dekker, *Phys. Rev. B* **61**, 2991 (2000).
  - [4] N. Hamada, S.-i. Sawada, and A. Oshiyama, *Phys. Rev. Lett.* **68**, 1579 (1992).
  - [5] R. Saito, M. Fujita, G. Dresselhaus, and M. S. Dresselhaus, *Phys. Rev. B* **46**, 1804 (1992).
  - [6] P. Kim, T. W. Odom, J.-L. Huang, and C. M. Lieber, *Phys. Rev. Lett.* **82**, 1225 (1999).
  - [7] L. C. Venema, J. W. Janssen, M. R. Buitelaar, J. W. G. Wildöer, S. G. Lemay, L. P. Kouwenhoven, and C. Dekker, *Phys. Rev. B* **62**, 5238 (2000).
  - [8] A. Loiseau, P. Launois, P. Petit, S. Roche, and J.-P. Salvetat, eds., *Understanding carbon nanotubes* (Springer, 2006).
  - [9] T. Ando, *J. Phys. Soc. Jpn* **66**, 1066 (1997).
  - [10] C. L. Kane and E. J. Mele, *Phys. Rev. Lett.* **90**, 207401 (2003).
  - [11] M. S. Dresselhaus, G. Dresselhaus, R. Saito, and A. Jorio, *Annu. Rev. Phys. Chem.* **58**, 719 (2007).
  - [12] T. Ando and U. Seiji, *Phys. Stat. Sol. (c)* **6**, 173 (2009).
  - [13] F. Wang, G. Dukovic, L. E. Brus, and T. F. Heinz, *Science* **308**, 838 (2005).
  - [14] G. Dukovic, F. Wang, D. Song, M. Y. Sfeir, T. F. Heinz, and L. E. Brus, *Nano Lett.* **5**, 2314 (2005).
  - [15] J. Maultzsch, R. Pomraenke, S. Reich, E. Chang, D. Prezzi, A. Ruini, E. Molinari, M. S. Strano, C. Thomsen, and C. Lienau, *Phys. Rev. B* **72**, 241402(R) (2005).
  - [16] C. L. Kane and E. J. Mele, *Phys. Rev. Lett.* **93**, 197402 (2004).
  - [17] J. Jiang, R. Saito, G. G. Samsonidze, A. Jorio, S. G. Chou, G. Dresselhaus, and M. S. Dresselhaus, *Phys. Rev. B* **75**, 035407 (2007).
  - [18] J. W. Janssen, S. G. Lemay, L. P. Kouwenhoven, and C. Dekker, *Phys. Rev. B* **65**, 115423 (2002).
  - [19] L. Vitali, M. Burghard, P. Wahl, M. A. Schneider, and K. Kern, *Phys. Rev. Lett.* **96**, 086804 (2006).
  - [20] R. Hesper, L. H. Tjeng, and G. A. Sawatzky, *Europhys. Lett.* **40**, 177 (1997).
  - [21] X. Lu, M. Grobis, K. H. Khoo, S. G. Louie, and M. F. Crommie, *Phys. Rev. B* **70**, 115418 (2004).
  - [22] J. D. Sau, J. B. Neaton, H. J. Choi, S. G. Louie, and M. L. Cohen, *Phys. Rev. Lett.* **101**, 026804 (2008).
  - [23] M. Ouyang, J.-L. Huang, C. L. Cheung, and C. M. Lieber, *Science* **292**, 702 (2001).
  - [24] T. Ando, *J. Phys. Soc. Jpn* **73**, 3351 (2004).